Defense Technical Information Center Compilation Part Notice

ADP010719

TITLE: NAL SST Arrow Wing with Oscillating Flap

DISTRIBUTION: Approved for public release, distribution unlimited

This paper is part of the following report:

TITLE: Verification and Validation Data for Computational Unsteady Aerodynamics [Donnees de verification et de valadation pour l'aerodynamique instationnaire numerique]

To order the complete compilation report, use: ADA390566

The component part is provided here to allow users access to individually authored sections of proceedings, annals, symposia, ect. However, the component should be considered within the context of the overall compilation report and not as a stand-alone technical report.

The following component part numbers comprise the compilation report:
ADP010704 thru ADP010735

12. NAL SST ARROW WING WITH OSCILLATING FLAP

M. Tamayama, K. Saitoh, H. Matsushita and J. Nakamichi

NAL, Tokyo

INTRODUCTION

A wind tunnel model of a SST(Supersonic Transport) arrow wing was tested in transonic regime. The purpose of this experiment is to accumulate verification data for the establishment of aeroelasticity related CFD codes and ACT (Active Control Technology) in the Japanese SST program.

The model is a semi-span arrow wing with a fuselage. The leading edge is double-swept-backed as shown in Fig. 1 and 2. The inboard sections of the model was constructed mainly with 7 mm thickness aluminum plate. A NACA0003 airfoil was, then, shaped by urethane resin. The dimensionless coordinates are shown in Table 1. At outboard sections, the NACA0003 airfoil was directly manufactured by cutting down an aluminum alloy. The detailed information on the model fuselage is shown in Table 2. Table 6 shows the model's natural frequencies acquired by both FEM analysis and a vibration test. Figure 5 shows the contours of model natural modes acquired by FEM analysis.

There is a flap, which can oscillate in the rear part of the inboard wing. The flap was driven by an electric motor around a hinge shaft which is parallel with the trailing edge. The deflection angle of the flap was measured using an appropriate transducer with installed inside the model fuselage. Downward motion was measured as positive angle.

Main measurement items presented here are pressures and deformations of the model. Steady and unsteady components of pressures were measured independently in order to remove the effect of thermal drift of pressure transducers. The pressure orifices are located at positions shown in Table 3 and Fig. 3. Chord positions in Table 3 are those for unsteady pressure transducers. The positions of steady pressure orifices are slightly different, because the span positions deviates 0.4% from the unsteady pressure orifices. The steady pressure orifice No.15 was not available because of the blockage of the vinyl tube, and it is not included in the experimental data provided.

The dynamic deformation of the model was measured by tracing optical targets installed in the wing surface. The positions of the optical targets are shown in Table 4 and Fig. 4. Multiple targets distributed in spanwise direction were measured with a single CCD camera. Four CCD cameras were used. While there were problems with the light intensity and some of the camera measurement systems failed, dynamic deformations were obtained at the target positions shown in Table 7.1. Four accelerometers are installed in the model. The locations are shown in Table 5 and Fig. 4. The accelerometer signals are useful for the verification of the dynamic deformation measurement system.

Tables 8.1 to 8.6 included in the accompanying CD-ROM show the results of steady and unsteady components of pressure coefficient, unsteady aerodynamic forces, steady and dynamic optical target displacement, and unsteady accelerometer signals. The unsteady results are presented only by the fundamental and 2nd harmonic components based on the flap frequency. The FFT function of Matlab was utilized in the frequency analysis. After data were FFT-processed in several intervals beginning from different time, they were averaged. The data length was double the sample frequency for each FFT-processing. The unsteady results presented in Tables 8.1 to 8.6 are not normalized by the flap amplitude. The phase characteristics are presented with respect to the flap motion. The results are also shown in Figs. 6, 7.1 to 7.12, 8.1, 8.2 and 9.1 to 9.6 (the whole set of figures is included in the accompanying CD-ROM here only some examples are presented). In these figures, only the fundamental component normalized by flap amplitude is shown.

LIST OF SYMBOLS AND DEFINITIONS

c	Local chord length
Cl	Unsteady section lift coefficient (normalized with c)
Cm	Unsteady section moment coefficient about 25% local chord (normalized with c^2)
c_{mean}	Mean geometrical chord length (1.27 m)
Cp	Steady pressure coefficient
c_r	Root chord length

f	Frequency
k	Reduced frequency. $f\pi c_{mean}/U$
M	Free stream Mach number
P	Unsteady Pressure above plenum chamber
P'	Real component of fundamental of P
P"	Imaginary component of fundamental of P
P1'	Real component of 2nd harmonic of P
P1"	Imaginary component of 2nd harmonic of P
Po	Free stream total pressure
q	Free stream dynamic pressure
Re	Reynolds number based on free stream conditions and c_r
s	Semi-span width
To	Free stream total temperature
U	Free stream velocity
x	Chordwise coordinate
y	Spanwise coordinate
z	Model deformation
z'	Real component of fundamental of z
z"	Imaginary component of fundamental of z
z1'	Real component of 2nd harmonic of z
z1"	Imaginary component of 2nd harmonic of z
α (alpha)	Angle of incidence
δ (delta)	Mean angle of flap deflection
δo (delta_o)	Amplitude of flap deflection
η (eta)	Dimensionless spanwise coordinate, y/s
Λ (lambda)	Sweepback angle
ξ (xi)	Dimensionless chordwise coordinate, x/c
θ (theta)	Phase lag of pressure with respect to flap motion

FORMULARY

1 General Description of model

1.1	Designation	NAL SST Arrow Wing with Fuselage
1.2	Type	Double swept-back semi-span model
1.3	Derivation	Proposed by Society of Japan Aircraft Company (SJAC).
1.4	Additional remarks	---
1.5	References	Ref. 1, 2

2 Model Geometry

2.1	Planform	Double tapered
2.2	Aspect ratio	2.01
2.3	Leading edge sweep	72.81 deg. (inboard) / 51.57 deg. (outboard)
2.4	Trailing edge sweep	6.57 deg. (inboard) / 16.94 deg. (outboard)
2.5	Taper ratio	$1.0_{\eta=0\%}$: $0.274_{57\%}$: $0.0783_{100\%}$
2.6	Twist	0
2.7	Wing root chord	2103.3 mm
2.8	Semi-span of model	1000.0 mm (From fuselage symmetry axis to wing tip. 35mm thickness base plate inserted between fuselage symmetry plane and tunnel side wall. See Table 2.)
2.9	Area of planform	0.8890 m^2 (only wing) [fuselage : 0.2778 m^2, base : 0.135 m^2]
2.10	Location of reference sections and definition of profiles	NACA0003 at 8 %, 57 % and 100 % semi-span positions (see Table 1)
2.11	Lofting procedure between reference sections	Straight line generators
2.12	Form of wing-body junction	Wing root supported from 52.8 % to 81.4 % chord-stations at 3 points (see Fig. 2). Rest of root free to deform, so it presented vertical displacements when the wing oscillated. A 1 mm clearance was thus given between fuselage and wing root section without any fairing.
2.13	Form of wing tip	Fairing using complex curve at 100 % semi-span position (semi-span length is slightly wider than 1000 mm. See Fig. 2)
2.14	Control surface details	Semi-span position : η=20.0 - 50.0 %
		Hinge-line : 110.0 mm upstream from trailing edge
		Small chordwise and spanwise gaps (see Ref. 1)
2.15	Additional remarks	Wing surface consist of aluminum alloy and urethane resin. Accuracy of wing section shape considered within 0.25 and 1.0 mm respectively for aluminum and urethane surfaces.
		Fuselage swell to cover the flap actuator presented in Table 2.
2.16	References	Ref. 1, 2

3 Wind Tunnel

3.1	Designation	NAL 2m x 2m transonic wind tunnel
3.2	Type of tunnel	Continuous and pressurized / depressurized
3.3	Test section dimensions	Height : 2000 mm, Width : 2000 mm Length : 4130 mm
3.4	Type of roof and floor	Slotted
3.5	Type of side walls	Closed
3.6	Ventilation geometry	6 slots on each of roof and floor. 6 % open ratio
3.7	Thickness of side wall boundary layer	ca. 0.1 m
3.8	Thickness of boundary layers at roof and floor	ca. 0.1 m (thicker than 0.1 m at slot sections)
3.9	Method of measuring Mach number	Derived from total and static pressures measured in settling and plenum chambers, respectively. Ratio of specific heats assumed 1.4.
3.10	Flow angularity	Less than 0.1 deg. (upwash).
3.11	Uniformity of Mach number over test section	Standard deviation of Mach number is less than 0.0025 for flow of Mach number less than 1.0.
3.12	Sources and levels of noise or turbulence in empty tunnel	At flow condition of M=0.7, Po=98kPa and To=310K, sound pressure levels based on $2x10^{-5}$ Pa are less than 130dB for each noise of 1st and 2nd fans and tunnel resonance.
3.13	Tunnel resonances	About 1 kHz corresponding to 1st natural frequency of test section plate.
3.14	Additional remarks	---
3.15	References on tunnel	Ref. 3 and 4 written in Japanese

4 Model motion

4.1	General description	Sinusoidal pitching of flap about swept hinge line
4.2	Definition of motion	Flap deflection angle relative to hinge line measured with a cam attached to hinge axis and a depth meter installed in fuselage.
4.3	Range of amplitude	Maximum command signal is 2 deg. with mean deflection angles of 0, 5 and -5 deg.
4.4	Range of frequency	0, 5, 10, 15(applied only to the mean deflection angle of 0 deg.), 20, 25 and 30 Hz
4.5	Method of applying motion	Forced by an electric motor
4.6	Timewise purity of motion	Adequate purity of sinusoid
4.7	Natural frequencies and normal modes of model and support system	First bending frequency at 9.79 Hz and second bending frequency at 40.25 Hz with 3 point support. Analytic and tested results shown in Table 6. Analytic natural modes presented in Fig. 5.
4.8	Actual mode of applied motion including any elastic deformation	Model dynamic deformation measured by observing optical targets installed in model. See Tables 8.1 to 8.6. Model 1st resonant frequency is almost 13.5 Hz with airflow. Flap oscillations at and below 15 Hz produce significant elastic deformations that influence unsteady pressure distributions and should be included in the calculations. Model deformation takes

		place most prominently in the 1st bending mode (Fig. 5). Detailed definition of the first 8 modes is included in the CD-ROM as file "FEM.txt"
4.9	Additional remarks	---
4.10	References	Ref. 1, 2

5 Test Conditions

5.1	Model planform area/tunnel area	0.222 (wing only). 0.325 (wing with fuselage and base plate)
5.2	Model span/tunnel width	0.500 (wing and fuselage). 0.518 (model with base plate)
5.3	Blockage	1.27%
5.4	Position of model in tunnel	Side mounted at middle height
5.5	Range of Mach number	0.80, 0.85, 0.90 and 0.95
5.6	Range of tunnel total pressure	70 and 80 kPa
5.7	Range of tunnel total temperature	306 to 315 deg. K
5.8	Range of model steady or mean incidence	-4, -3, -2, -1, 0, 1 and 2 deg.
5.9	Definition of model incidence	Model set to zero incidence in horizontal plane.
5.10	Position of transition, if free	Not measured
5.11	Position and type of trip, if transition fixed	---
5.12	Flow instabilities during tests	No remarkable instabilities detected.
5.13	Changes to mean shape of model due to steady aerodynamic load	About 7.5 mm wing tip displacement at M=0.85 and Po=80 kPa. See Tables 8.1 to 8.6.
5.14	Additional remarks	---
5.15	References describing tests	---

6 Measurements and Observations

6.1	Steady pressures for the mean conditions	Available
6.2	Steady pressures for small changes from the mean conditions	Not Available
6.3	Quasi-steady pressures	Not Available
6.4	Unsteady pressures	Available
6.5	Steady section forces for the mean conditions by integration of pressures	Not Available
6.6	Steady section forces for small changes from the mean conditions by integration	Not Available
6.7	Quasi-steady section forces by integration	Not Available
6.8	Unsteady section forces by integration	Available
6.9	Measurement of actual motion at points of model	Available
6.10	Observation or measurement of boundary layer properties	Not Available
6.11	Visualisation of surface flow	Not Available
6.12	Visualisation of shock wave movements	Not Available
6.13	Additional remarks	Accelerometer signals also measured.

6.14 References	Ref. 2

7 Instrumentation

7.1 Steady pressure	
7.1.1 Position of orifices	See Table 3 and Fig. 3
7.1.2 Type of measuring system	Orifices connected to scannivalves through vinyl tubes.
7.2 Unsteady pressure	
7.2.1 Position of orifices	See Table 3 and Fig. 3
7.2.2 Diameter of orifices	1.0 mm
7.2.3 Type of measuring system	Individual in situ transducers
7.2.4 Type of transducers	Kulite XCS-062 range 15 PSI
7.2.5 Principle and accuracy of calibration	Steady calibration against DPI601 using reference tube of pressure transducer. Accuracy of the device is 0.05%.
7.3 Model motion	
7.3.1 Method of measuring motion reference coordinates	Distance measured by depth meter mounted in fuselage and cam attached to hinge root.
7.3.2 Method of determining spatial mode of motion	Not measured for flap, but for wing itself. Optical targets set in the model were traced with CCD cameras. The position of targets presented in Table 4 and Fig. 4.
7.3.3 Accuracy of measured motion	Time response of angular transducer is less than 1 msec, which is equal to 10.8 deg. phase lag at 30 Hz flap motion. Accuracy of magnitude is less than 1 % taking into account non-linearity of depth meter and cam, and temperature characteristics of depth meter and its amplifier.
7.4 Processing of unsteady measurements	
7.4.1 Method of acquiring and processing measurements	Pressure above the plenum chamber, accelerometer signal, flap control signal and its actual motion sampled simultaneously at 25.6 kHz and stored. Data processed off-line to 256 Hz. Dynamic model deformation measured by another system at 333 Hz and stored.
7.4.2 Type of analysis	Complex components of Cp using about 5 seconds data for each flap frequency. Averaging conducted. See INTRODUCTION.
7.4.3 Unsteady pressure quantities obtained and accuracies achieved	Fundamental and 2nd harmonic components for each flap frequency presented. Although no unsteady calibrations were conducted, accuracy shown in 9.1.6 is expected.
7.4.4 Method of integration to obtain forces	Simpson method. Discretely divided distributions using spline interpolation. Leading edge unsteady Cp assumed to zero. At outboard section, trailing edge unsteady Cp assumed to mean of values extrapolated on each of upper and lower surfaces.
7.5 Additional remarks	4 accelerometers installed in wing (see Table 5 and Fig. 4).
7.6 References on techniques	Ref. 1

8 Data presentation

8.1 Test cases for which data could be made available	Table 7.2 (Included in accompanying CD-ROM)

8.2	Test cases for which data are included in this document	Table 7.1
8.3	Steady pressures	Tables 8.1 to 8.6 (Included in accompanying CD-ROM)
8.4	Quasi-steady or steady perturbation pressures	---
8.5	Unsteady pressures	Tables 8.1 to 8.6 (Included in accompanying CD-ROM)
8.6	Steady forces or moments	---
8.7	Quasi-steady or unsteady perturbation forces	---
8.8	Unsteady forces and moments	Tables 8.1 to 8.6 (Included in accompanying CD-ROM)
8.9	Other forms in which data could be made available	Static and dynamic model deformations presented in Tables 8.1 to 8.6. Accelerometer signals also presented in Tables 8.1 to 8.6.
8.10	Reference giving other representations of data	---

9 Comments on data

9.1	Accuracy	
	9.1.1 Mach number	Less than 0.001
	9.1.2 Steady incidence	0.1 deg.
	9.1.3 Reduced frequency	Less than 0.12%
	9.1.4 Steady pressure coefficients	Less than $(7.9\times Cp^2 + 5.9)^{0.5} \times 0.001$
	9.1.5 Steady pressure derivatives	---
	9.1.6 Unsteady pressure coefficients	Accuracy of $\mid P/q \mid$ less than $(0.22\times\mid P/q\mid^2 + 1.2)^{0.5} \times 0.01$. Effects of repeatability and temperature sensitivity of pressure transducer and calibration error were considered.
9.2	Sensitivity to small changes of parameter	Not examined
9.3	Non-linearities	Expansion waves seemed to appear only on the flap at higher Mach number. Unsteady pressure distribution affected by non-linearity of dynamic model deformation at model 1st resonant frequency.
9.4	Influence of tunnel total pressure	Total pressure of 70 and 80 kPa examined.
9.5	Effects on data of uncertainty, or variation, in mode of model motion	Not estimated yet
9.6	Wall interference corrections	None
9.7	Other relevant tests on same model	Ref. 1
9.8	Relevant tests on other models of nominally the same shapes	---
9.9	Any remarks relevant to comparison between experiment and theory	---
9.10	Additional remarks	---
9.11	References on discussion of data	Ref. 2

10 Personal contact for further information

Masato Tamayama

Aeroelasticity Laboratory, Structures Division

National Aerospace Laboratory

7-44-1, Jindaiji-Higashi-Machi,
Chofu, Tokyo 182-8522, JAPAN
Phone : +81-422-40-3392
Fax : +81-422-40-3376
E-mail : masato@nal.go.jp

11 List of references

1 M. Tamayama, H. Miwa, J. Nakamichi; Unsteady Aerodynamics Measurements on an Elastic Wing Model of SST, AIAA 97-0836, 1997

2 M. Tamayama, K. Saitoh, H. Matsushita; Measurements of Unsteady Pressure Distributions and Dynamic Deformations on an SST Elastic Wing Model, CEAS International Forum on Aeroelasticity and Structural Dynamics, Rome, Italy, 1997, Vol.3, pp.231-238.

3 N. Kawai, Y. Oguni, M. Suzuki; Measurements of Free-Stream Turbulence and Disturbance in NAL 2m x 2m Transonic Windtunnel, NAL TM-342, 1978 (in Japanese).

4 K. Suzuki, et al; Refurbishment of the NAL 2m x 2m Transonic Wind Tunnel Test Section, NAL TM-674, 1995 (in Japanese).

Table 1 Airfoil Section Shape

Airfoil NACA0003

$z_t(\xi) / c = 5 \times 0.03 \times \{ a_0\xi^{1/2} + a_1\xi + a_2\xi^2 + a_3\xi^3 + a_4\xi^4 \}$

$a_0 = 0.2969$, $a_1 = -0.1260$, $a_2 = -0.3516$

$a_3 = 0.2843$, $a_4 = -0.1015$

$z_t(\xi)$:Local airfoil thickness

ξ	$z_t(\xi)$	ξ	$z_t(\xi)$
0.00	0.00000	0.52	0.01291
0.04	0.00807	0.56	0.01220
0.08	0.01077	0.60	0.01141
0.12	0.01247	0.64	0.01055
0.16	0.01360	0.68	0.00964
0.20	0.01434	0.72	0.00867
0.24	0.01478	0.76	0.00764
0.28	0.01498	0.80	0.00656
0.32	0.01498	0.84	0.00542
0.36	0.01482	0.88	0.00423
0.40	0.01451	0.92	0.00299
0.44	0.01408	0.96	0.00168
0.48	0.01354	1.00	0.00031

Table 2 Definition of Fuselage

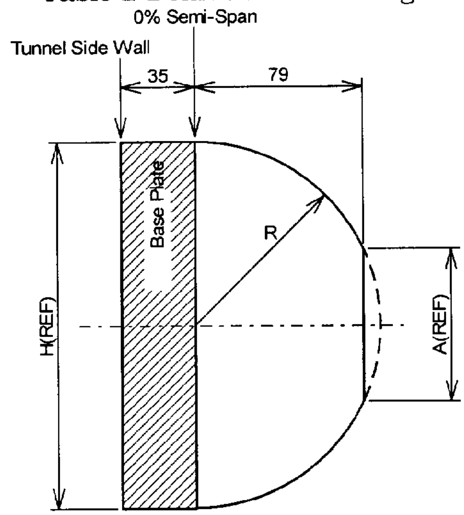

(unit : mm)

STA	R	H(REF)	A(REF)
-760	0.00	0.00	-----
-700	15.31	30.63	-----
-600	36.65	73.31	-----
-500	53.27	106.54	-----
-400	65.76	131.52	-----
-300	74.71	149.42	-----
-200	80.71	161.41	33.02
-100	84.34	168.69	59.10
0	86.21	172.43	69.04
100	86.90	173.80	72.41
190	87.00	174.00	72.88
200 : 1700	87.00	174.00	72.88
1824.4 : 2204.4	*(control surface actuator swell)		
2300 : 2400	87.00	174.00	72.88
2500	86.62	173.24	71.05
2600	84.04	168.08	57.32
2700	78.02	156.04	-----
2800	68.56	137.12	-----
2900	55.52	111.04	-----
3000	37.32	74.64	-----
3100	0.00	0.00	-----

The origin of STA is the wing leading edge
at 8% semi-span position (wing-fuselage junction).

*(control surface actuator swell)

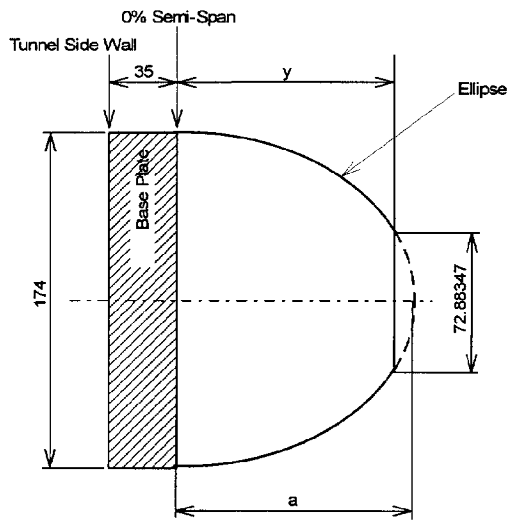

(unit : mm)

STA	y	a
1824.4	80.00	88.10
1864.4	85.50	94.16
1904.4	95.50	105.17
1944.4	109.50	120.59
1984.4	115.00	126.64
2024.4	114.00	125.54
2064.4	107.00	117.83
2104.4	94.00	103.52
2144.4	84.00	92.51
2184.4	80.00	88.10
2204.4	79.50	87.55

Table 3 Pressure Orifice Locations

η= 38.4% span (Steady) 38% span (Unsteady)				η= 73.5% span (Steady) 73.9% span (Unsteady)			
Upper Surface		Lower Surface		Upper Surface		Lower Surface	
ch	x/c [%]	ch	x/c [%]	ch	x/c [%]	ch	x/c [%]
1	2.5	22	70.0	30	10.0	39	79.0
2	5.0	23	60.0	31	20.0	40	66.0
3	7.5	24	50.0	32	30.0	41	54.2
4	10.0	25	40.0	33	35.0	42	48.0
5	15.0	26	30.0	34	41.8	43	41.8
6	20.0	27	20.0	35	48.0	44	30.0
7	30.0	28	10.0	36	54.2	45	20.0
8	40.0	29	5.0	37	66.0	46	10.0
9	50.0			38	80.0		
10	60.0						
11	70.0						
12	80.0						
13	82.5						
14	85.0						
15	86.5*						
16	88.0						
17	91.6						
18	93.1						
19	94.6						
20	96.1						
21	100.0*						

* : Only for Unsteady Measurement

Table 4 Optical Target Locations

No.	η %	ξ %	No.	η %	ξ %
* 1	96.0	13.0	11	41.0	43.2
* 2	96.0	38.6	12	41.0	63.2
3	96.0	64.2	* 13	41.0	74.0
4	76.0	28.2	* 14	41.0	83.4
* 5	76.0	48.5	15	18.0	38.2
* 6	76.0	66.3	16	18.0	59.9
7	60.0	3.4	* 17	18.0	73.0
8	60.0	41.4	* 18	18.0	80.2
* 9	60.0	59.1	* 19	18.0	87.1
10	41.0	5.0	* 20	60.0	74.5
			21	18.0	20.6

* Available

Table 5 Position of Accelerometers

66.8% Semi-Span		84.7% Semi-Span	
No.	% x/c	No.	% x/c
1	30.0	2	30.0
3	65.0	4	65.0

Table 6 Model Natural Frequencies

Mode	Natural Frequency[Hz]		Generalized Mass [kg]
	FEM	Vibration Test	
1	11.09	9.79	5.1982
2	41.65	---	2.3109
3	44.00	40.25	3.2874
4	56.26	47.91	1.9764
5	89.49	65.19	1.4333
6	119.23	90.57	0.7928
7	145.44	111.04	2.0683
8	163.58	122.39	1.2810

Table 7.1 SUMMARY OF PRESENTED DATA

Test ID No.	M	Po [kPa]	To [°K]	Re x 10^{-7}	k/f [/Hz]	f [Hz]	α [°]	δ [°]	Target data available
AC100803	0.8002	79.925	310.36	2.142	0.0150	5, 10, 15, 20, 25, 30	0	0	1, 2, 5, 6, 9, 13, 14, 18, 19, 20
AC100804	0.8004	79.963	310.52	2.141	0.0150	5, 10, 20, 25, 30	0	5	1, 2, 5, 6, 9, 20
AC100901	0.8507	80.000	310.34	2.207	0.0143	5, 10, 15, 20, 25, 30	0	0	1, 2, 5, 6, 9, 13, 14, 17, 18, 19, 20
AC100902	0.8489	79.936	310.78	2.199	0.0143	5, 10, 20, 25, 30	0	-5	1, 2, 5, 6, 9, 13, 14, 17, 18, 19, 20
AC100907	0.9001	80.083	311.87	2.247	0.0135	5, 10, 15, 20, 25, 30	0	0	1, 2, 5, 6, 9, 13, 14, 17, 18, 19, 20
AC100908	0.9005	79.956	312.34	2.239	0.0135	5, 10, 20, 25, 30	0	5	1, 2, 5, 6, 9, 13, 17, 18, 20

Table 8.1 Result / AC100803

```
| Test No. AC100803                                     |
| M = 0.8002,  Po = 79.925 kPa,  To = 310.36 deg. K    |
| Re = 2.142*10^7,  k/f = 0.0150 /Hz                    |
| Alpha =  0 deg.,  Delta =  0 deg.                     |
~~~~~~~~~~~~~~~~~~~~~~~~~~~~~~~~~~~~~~~~~~~~~~~~~~~~~~~~~
```

[STEADY DATA]

< PRESSURE COEFFICIENT (Cp) >

Eta = 38.4%

Upper surface Orifice No.	Xi	Cp	Lower surface Orifice No.	Xi	Cp
1	0.025	-0.0229	22	0.700	-0.0458
2	0.050	-0.0400	23	0.600	-0.0551
3	0.075	-0.0420	24	0.500	-0.0605
4	0.100	-0.0440	25	0.400	-0.0545
5	0.150	-0.0496	26	0.300	-0.0600
6	0.200	-0.0571	27	0.200	-0.0529
7	0.300	-0.0613	28	0.100	-0.0403
8	0.400	-0.0667	29	0.050	-0.0563
9	0.500	-0.0573			
10	0.600	-0.0494			
11	0.700	-0.0426			
12	0.800	-0.0222			
13	0.825	-0.0327			
14	0.850	-0.0368			
16	0.880	-0.0235			
17	0.900	-0.0338			
18	0.920	-0.0211			
19	0.950	-0.0138			
20	0.970	+0.0447			

Eta = 73.5%

Upper surface Orifice No.	Xi	Cp	Lower surface Orifice No.	Xi	Cp
30	0.100	-0.1239	39	0.790	-0.0149
31	0.200	-0.1254	40	0.660	-0.0479
32	0.300	-0.0941	41	0.542	-0.0532
33	0.350	-0.0848	42	0.480	-0.0622
34	0.418	-0.0785	43	0.418	-0.1022
35	0.480	-0.0695	44	0.300	-0.1081
36	0.542	-0.0702	45	0.200	-0.1247
37	0.660	-0.0492	46	0.100	-0.1151
38	0.800	-0.0448			

< DEFORMATION FROM NO-FLOW CONDITION >

Target NO.	
1	+8.9354e-003
2	+9.2979e-003
5	+6.6282e-003
6	+6.9474e-003
9	+4.5407e-003
13	+2.4733e-003
18	+9.0811e-004
19	+1.2350e-003
20	+4.9521e-003
	[unit : m]

[UNSTEADY DATA]

f = 5.0 Hz Delta_o = 1.407 deg.

< PRESSURE >

No.	P'/q	P''/q	Pl'/q	Pl''/q	No.	P'/q	P''/q	Pl'/q	Pl''/q
1	+7.8672e-004	+4.3709e-005	+8.0516e-005	-5.8224e-005	24	-1.1412e-003	+4.8577e-005	-3.5234e-004	-5.9388e-005
2	+7.5615e-004	+3.6843e-005	+8.3223e-005	-5.1448e-005	25	-1.1946e-003	+9.3217e-005	-3.3515e-004	-4.4607e-005
3	+7.2296e-004	+1.7149e-005	+9.1091e-005	-2.5512e-005	26	-9.6874e-004	+5.0285e-005	-2.5858e-004	-3.5429e-005
4	+7.1944e-004	+5.0864e-005	+8.6095e-005	-5.9453e-005	27	-7.9342e-004	+5.6215e-005	-2.2098e-004	-3.3815e-005
5	+8.0283e-004	+3.0358e-005	+1.2223e-004	-8.6025e-005	28	-8.8828e-004	+6.7967e-005	-1.9143e-004	-2.8182e-005
6	+6.6100e-004	+7.0002e-005	+1.2902e-004	-8.9684e-005	29	-7.8033e-004	+4.7247e-005	-1.6621e-004	-3.8227e-005
7	+1.0015e-003	+1.0361e-004	+1.3800e-004	-8.1173e-005	30	+4.6798e-003	+2.3276e-004	+9.8975e-004	-9.0601e-005
8	+1.3027e-003	+6.1052e-005	+2.1992e-004	-1.1785e-004	31	+1.9328e-003	+1.4899e-004	+5.4238e-004	-6.5775e-005
9	+1.1805e-003	+8.9660e-005	+2.1234e-004	-1.0954e-004	32	+9.2340e-005	+1.4845e-004	+2.0084e-004	-7.4948e-005
10	+7.8312e-004	+3.6655e-005	+1.5814e-004	-1.1425e-004	33	-3.8883e-004	+1.4808e-004	+1.9665e-004	-1.0070e-004
11	-9.8334e-004	-1.0328e-004	-7.1924e-005	-2.0106e-004	34	-9.4809e-004	+1.0313e-004	+9.0647e-005	-1.1219e-004
12	-5.7040e-003	-6.1674e-004	-7.0427e-004	-4.4130e-004	35	-1.5268e-003	+1.0638e-004	-3.5361e-006	-9.9731e-005
13	-8.5204e-003	-6.2376e-004	-1.0955e-003	-4.4207e-004	36	-1.9714e-003	+9.2792e-005	-6.7405e-005	-1.1752e-004
14	-1.2701e-002	-1.0577e-003	-1.6996e-003	-5.5173e-004	37	-1.9822e-003	+7.4661e-005	-4.9516e-005	-1.4588e-004
15	-1.6012e-002	-1.3849e-003	-2.1815e-003	-6.0164e-004	38	-1.5498e-003	+8.7056e-005	-9.5056e-005	-1.3375e-004
16	-2.7111e-002	-2.5209e-003	-3.8842e-003	-8.6146e-004	39	+1.5977e-003	+2.0498e-004	-6.9301e-005	-1.3918e-004
17	-6.5368e-002	-4.4412e-003	-5.8103e-003	-1.5791e-003	40	+2.0575e-003	+2.2058e-004	-6.3125e-005	-1.3469e-004
18	-4.1524e-002	-3.3402e-003	-4.1162e-003	-1.1320e-003	41	+1.9475e-003	+1.8157e-004	-1.2719e-004	-1.4087e-004
19	-2.7545e-002	-2.5878e-003	-2.8568e-003	-9.0288e-004	42	+1.5229e-003	+1.6212e-004	-2.1213e-004	-1.4390e-004
20	-1.7642e-002	-1.9067e-003	-1.9389e-003	-7.1725e-004	43	+1.0206e-003	+1.0437e-004	-3.2457e-004	-1.5941e-004
21	+1.5456e-004	+2.1606e-004	+2.1787e-004	-6.7360e-005	44	-4.6880e-004	+7.7942e-005	-5.3641e-004	-1.5246e-004
22	+7.3478e-004	+2.3072e-004	-1.9087e-004	-1.9774e-006	45	-2.0729e-003	+3.9180e-005	-7.7220e-004	-1.8623e-004
23	-9.1626e-004	+9.5325e-005	-3.8716e-004	-6.6705e-005	46	-4.9538e-003	-4.0297e-005	-1.3125e-003	-2.3554e-004

< AERODYNAMIC FORCE >

	real(fundamental)	imag(fundamental)	real(2nd harmonic)	imag(2nd harmonic)
Cl inboard	+4.4811e-003	+5.4617e-004	+3.0432e-004	+2.4205e-004
Cl outboard	+1.9189e-004	-2.9888e-006	-5.3971e-004	-4.7549e-005
Cm inboard	-3.5334e-003	-3.4665e-004	-3.4419e-004	-1.3376e-004
Cm outboard	-9.4222e-004	-2.7897e-005	-4.0941e-005	+3.2761e-007

< DYNAMIC DEFORMATION >

Target NO.	real(fundamental)	imag(fundamental)	real(2nd harmonic)	imag(2nd harmonic)
1	+3.0206e-003	-5.5430e-005	+2.9867e-004	-5.6899e-004
2	+3.1819e-003	-5.8974e-005	+3.1358e-004	-5.9964e-004
5	+2.3323e-003	-2.5983e-004	+1.4506e-004	-4.6065e-004
6	+2.5142e-003	-4.4531e-005	+2.4202e-004	-4.5089e-004
9	+1.7175e-003	-1.9038e-004	+1.0799e-004	-3.2052e-004
13	+9.6971e-004	-1.0812e-004	+5.9302e-005	-1.7505e-004
14	+1.1849e-003	-1.3701e-004	+6.6696e-005	-2.1126e-004
18	+2.1879e-004	-2.4470e-005	+1.4574e-005	-3.7917e-005
19	+3.6009e-004	-5.5330e-005	+1.9597e-005	-5.7822e-005
20	+1.9133e-003	-2.1409e-004	+1.1434e-004	-3.5716e-004

[unit : m]

< ACCELERATION >

Acc. NO.	real(fundamental)	imag(fundamental)	real(2nd harmonic)	imag(2nd harmonic)
1	-1.6517e+000	-1.0160e-001	-1.3742e+000	-1.0738e-001
2	-2.6439e+000	-1.7970e-001	-2.2206e+000	-1.5267e-001
3	-1.8257e+000	-4.7501e-002	-1.6589e+000	-1.1162e-001
4	-2.8493e+000	-1.5522e-001	-2.4137e+000	-1.4551e-001

[unit : m/s^2]

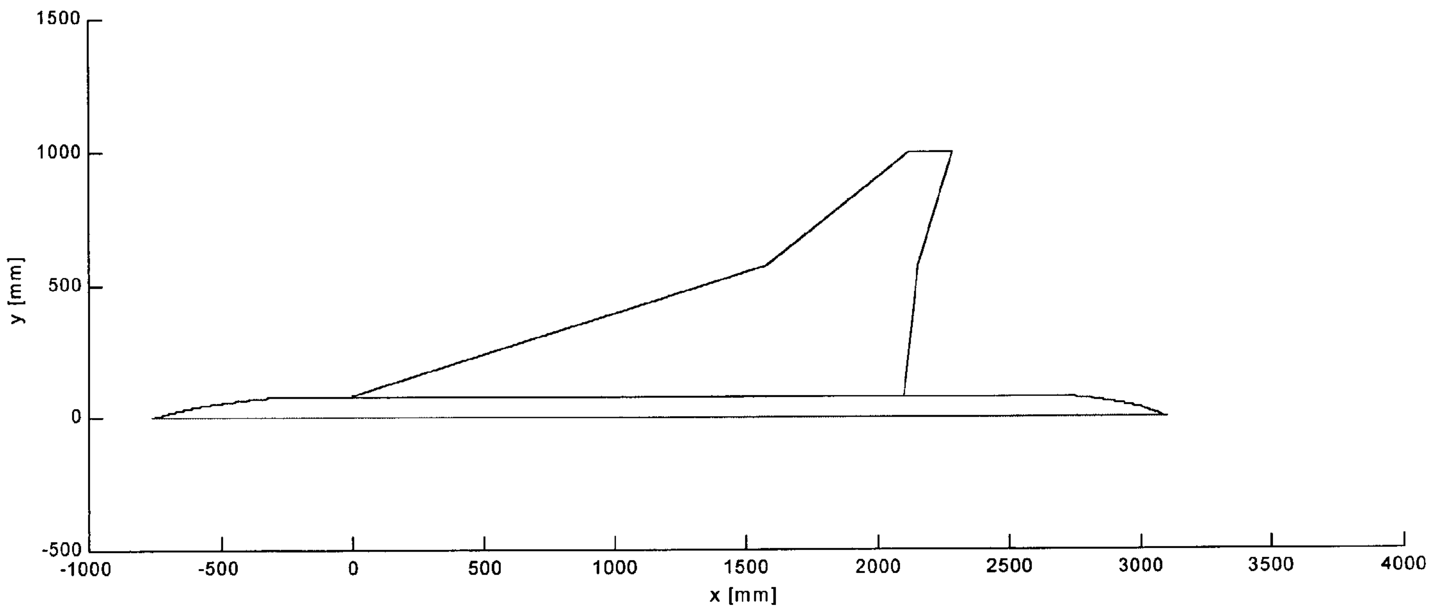

Figure 1 Semi-span Planform of SST Arrow Wing Model

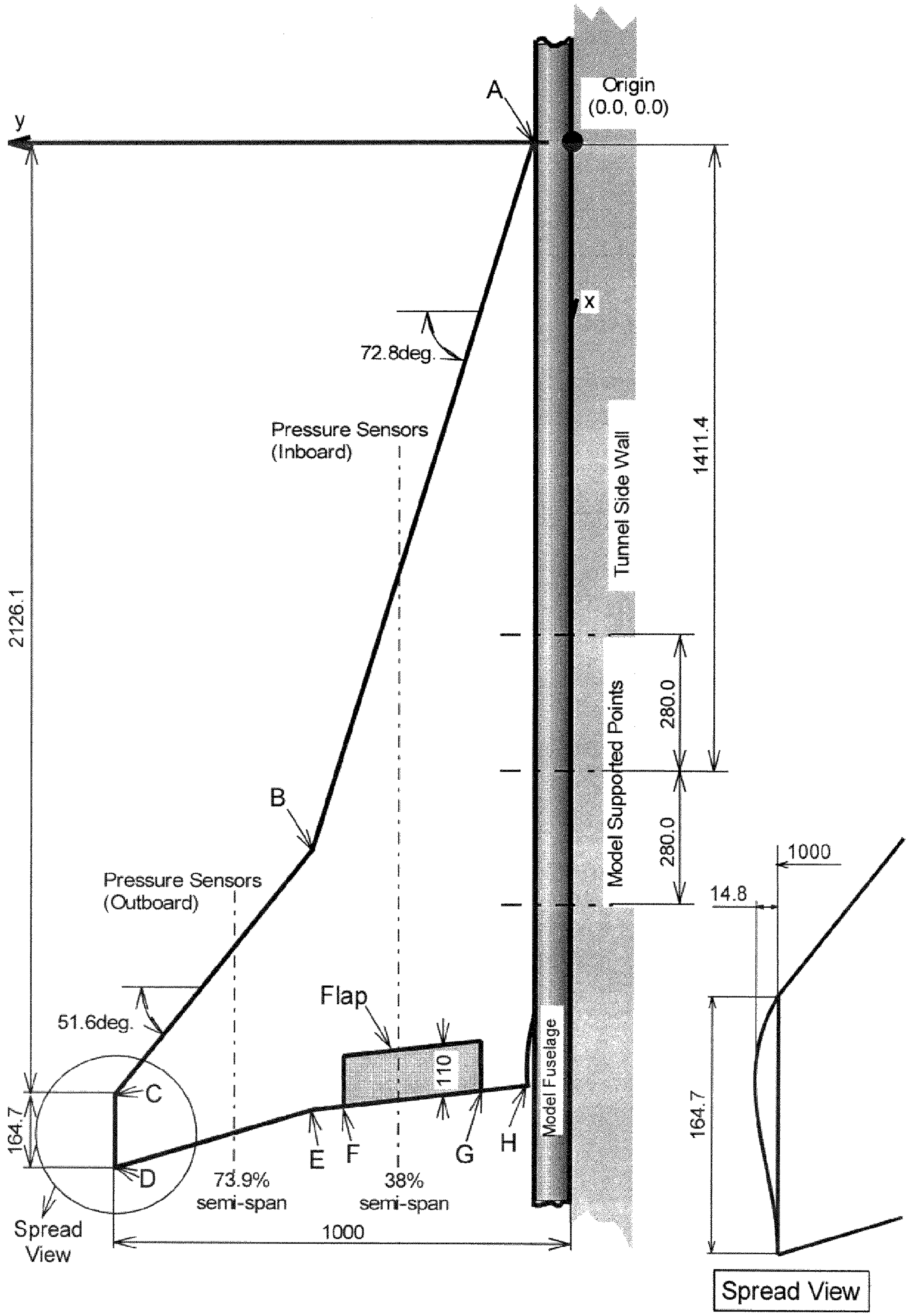

Figure 2 Model Planform (wing part)

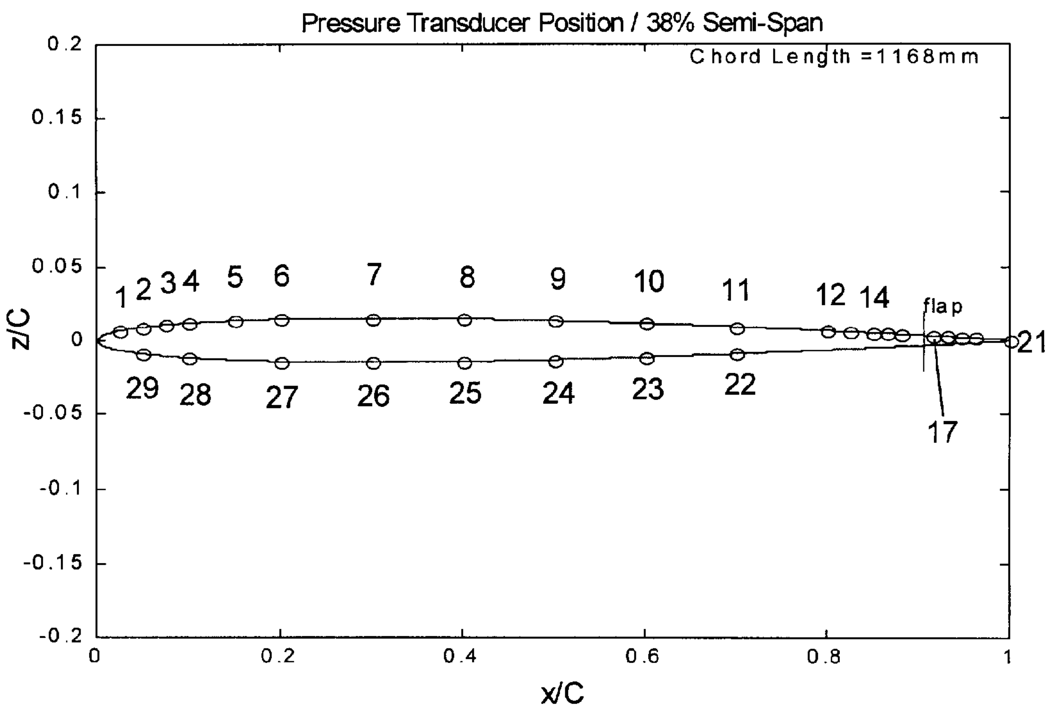

(a) 38 % semi-span

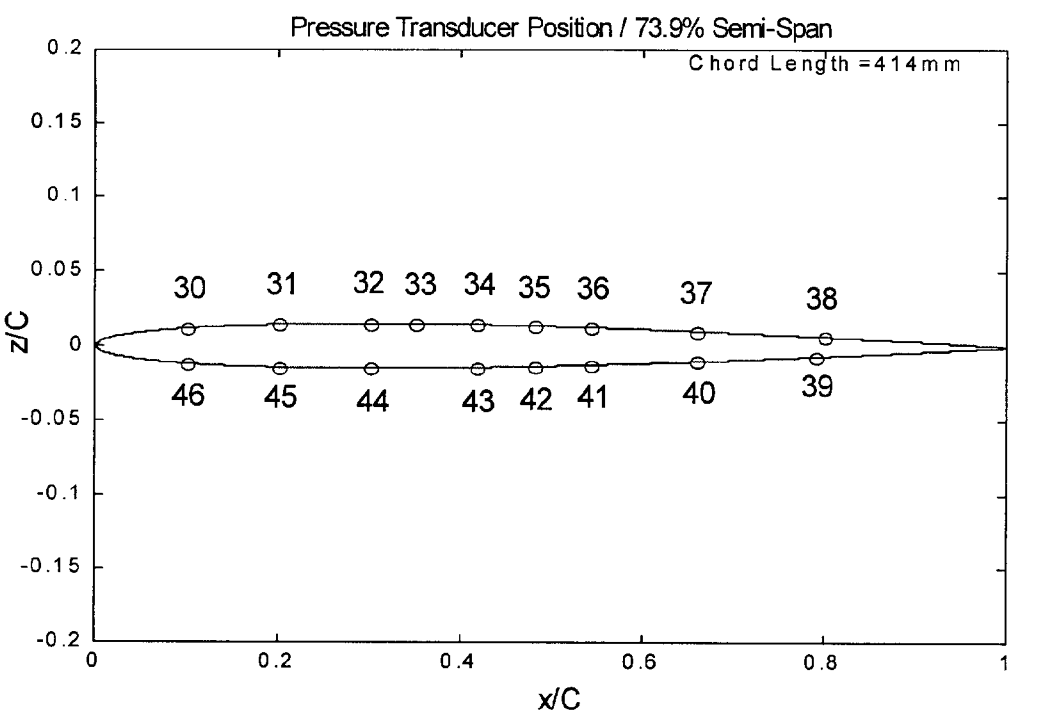

(b) 73.9 % semi-span

Figure 3 Pressure Orifice Positions

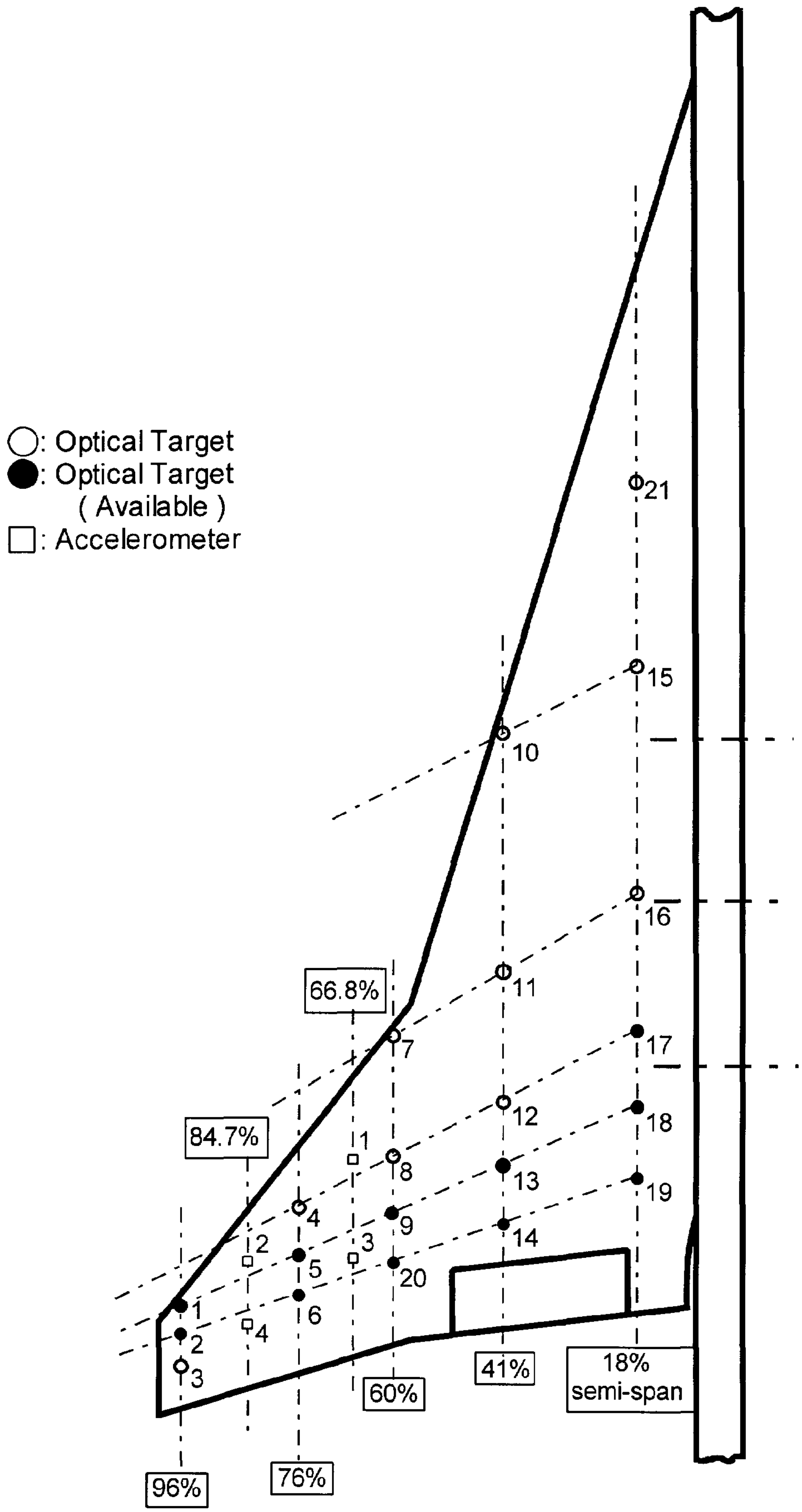

Figure 4 Positions of Optical Targets

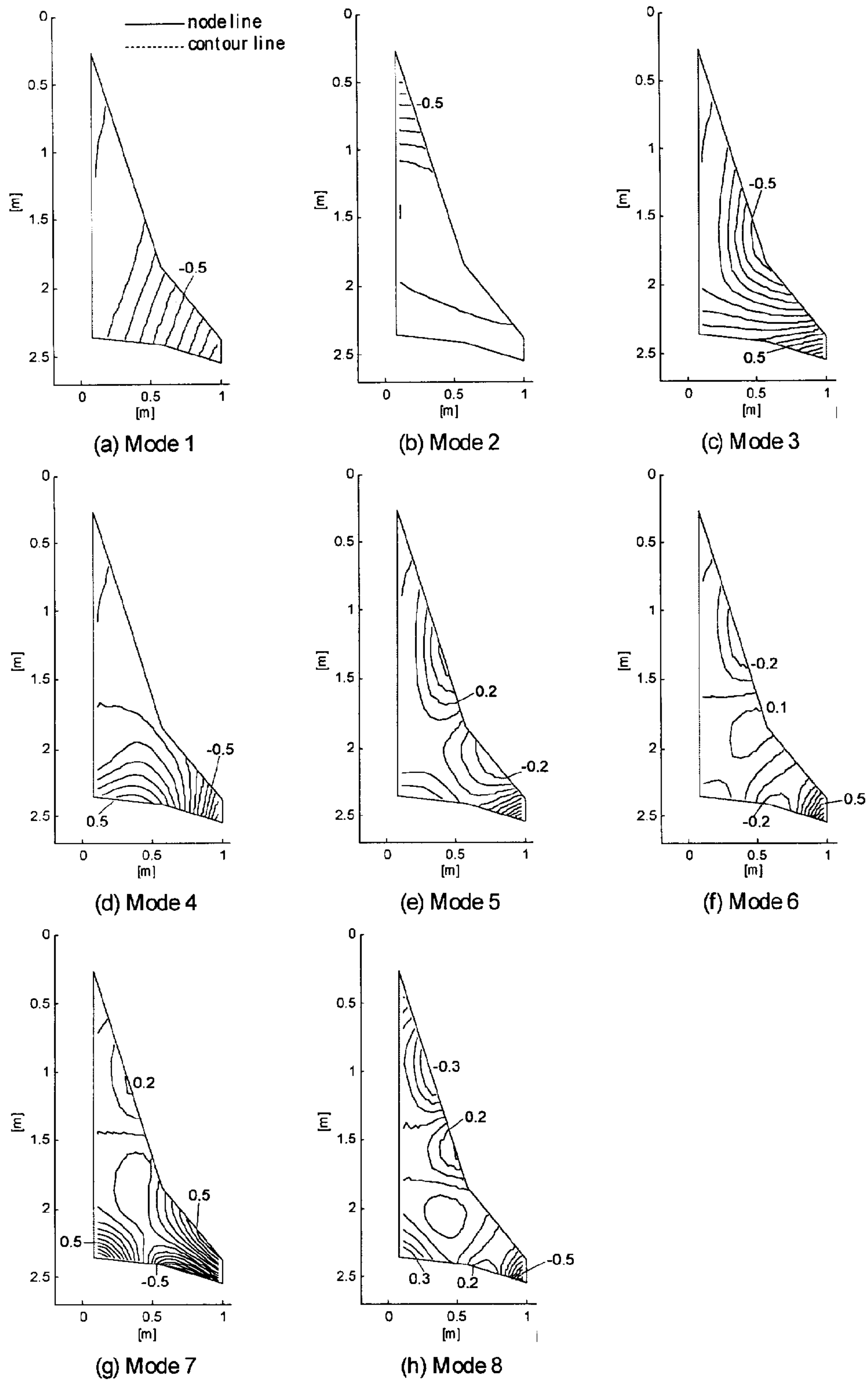

Figure 5 Model Natural Mode Contours Acquired by FEM
(Contours are normalized with the maximum displacement)

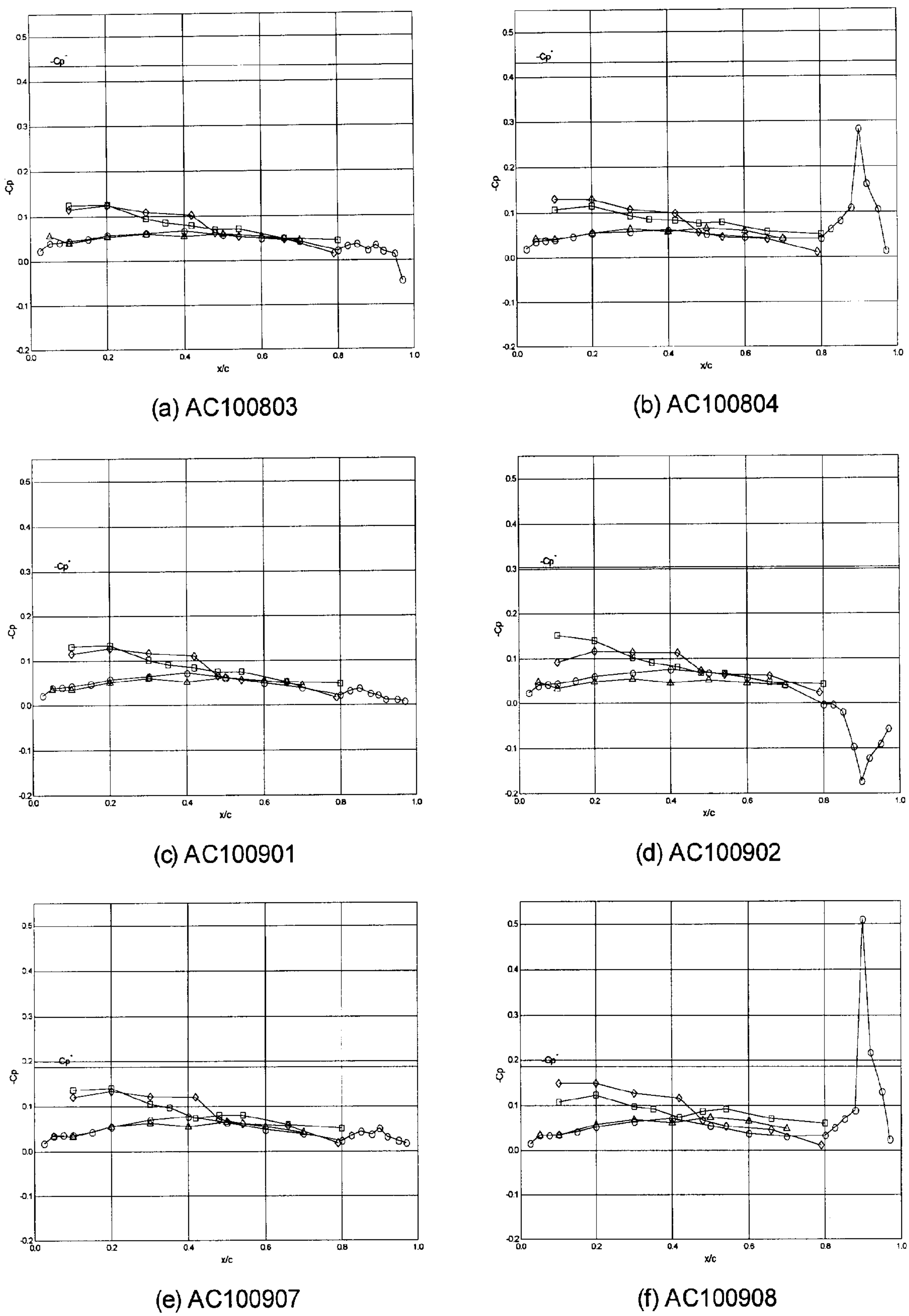

(a) AC100803

(b) AC100804

(c) AC100901

(d) AC100902

(e) AC100907

(f) AC100908

Figure 6 Steady Pressure Coefficient Distributions.
(O: Inboard Upper , Δ: Lower , □: Outboard Upper, ◊: Lower)

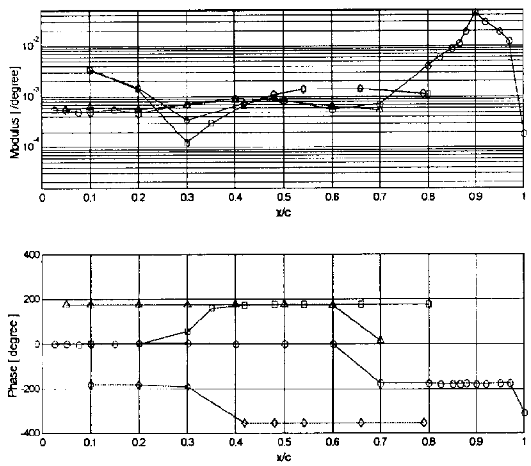

(a) f = 5 [Hz]

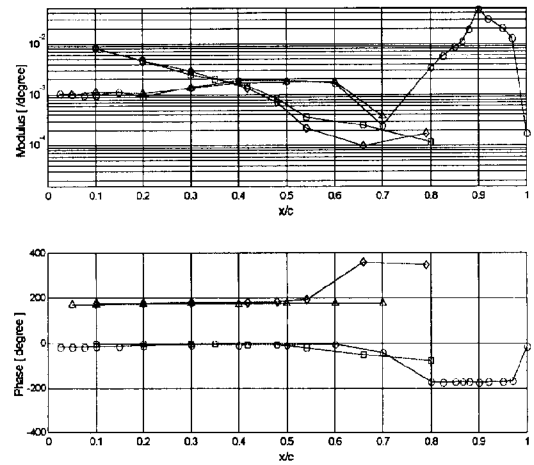

(b) f = 10 [Hz]

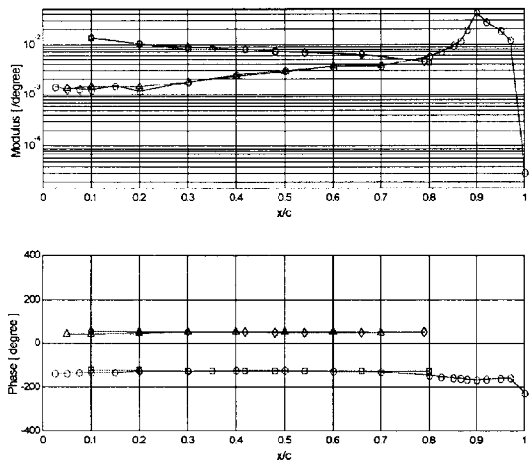

(c) f = 15 [Hz]

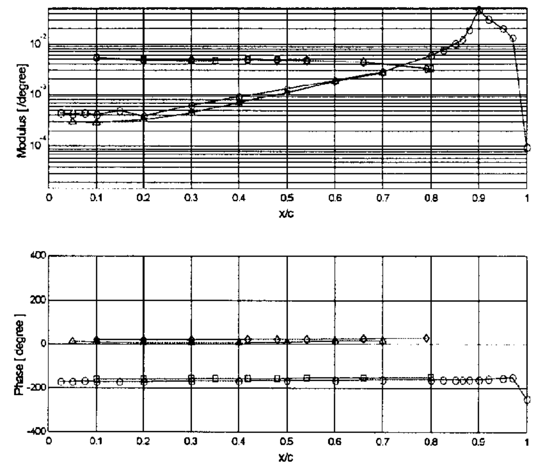

(d) f = 20 [Hz]

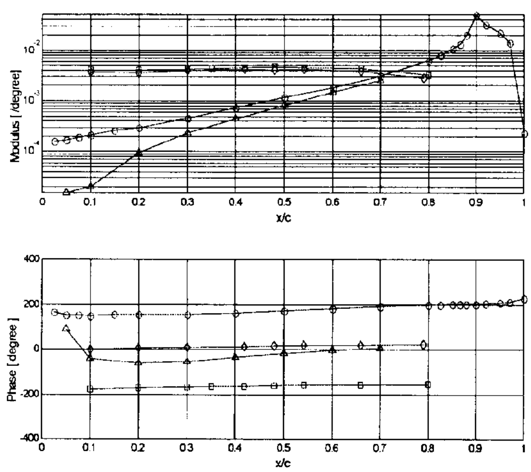

(e) f = 25 [Hz]

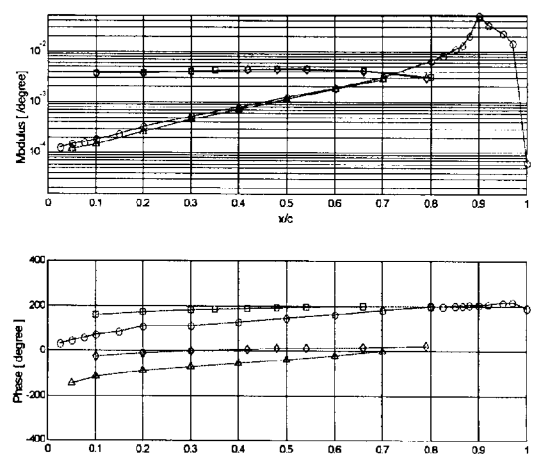

(f) f = 30 [Hz]

Figure 7.1 Unsteady Pressure Distributions. x/c vs Modulus & Phase.
Test Case AC100803 M = 0.8002, Po = 79.925 kPa,
Re = $2.142 * 10^7$, Alpha = 0 deg., Delta = 0 deg.
(O: Inboard Upper , Δ: Lower , □: Outboard Upper, ◊: Lower)

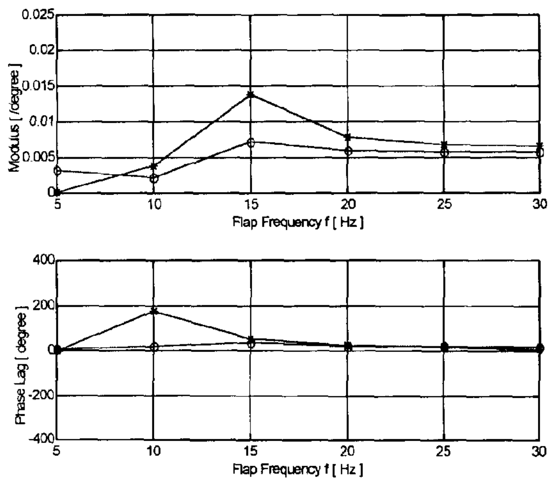

(a) AC100803, M=0.8002, Cl

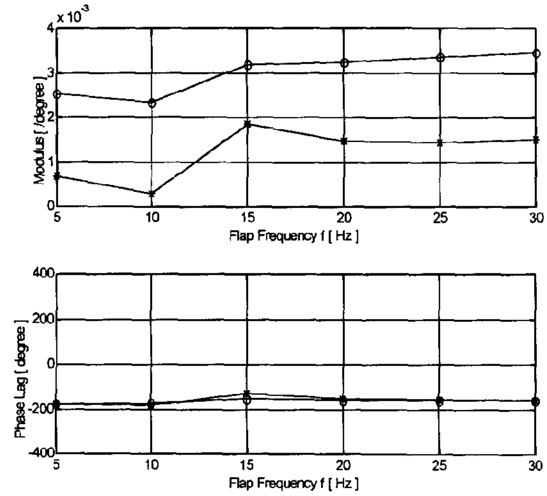

(b) AC100803, M=0.8002, Cm

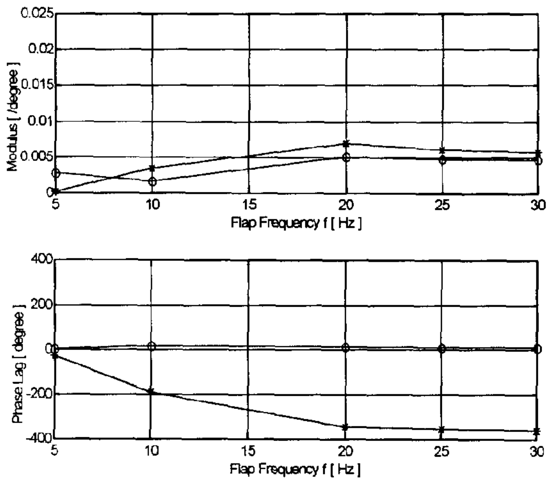

(c) AC100804, M=0.8004, Cl

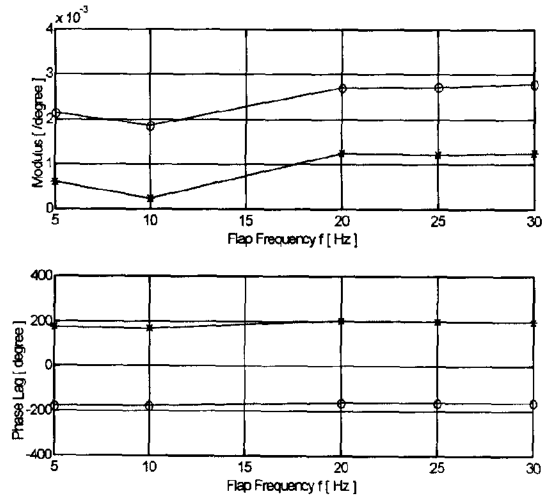

(d) AC100804, M=0.8004, Cm

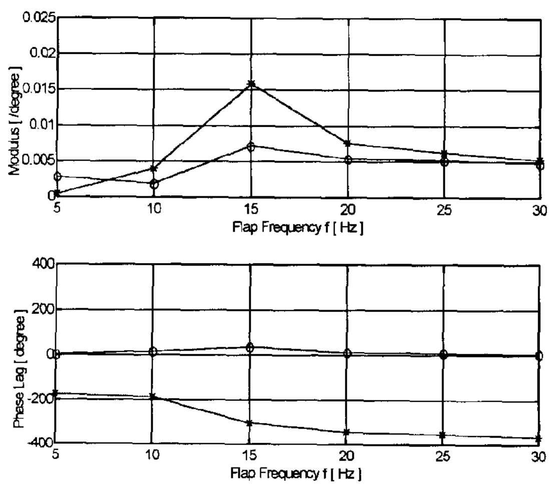

(e) AC100901, M=0.8507, Cl

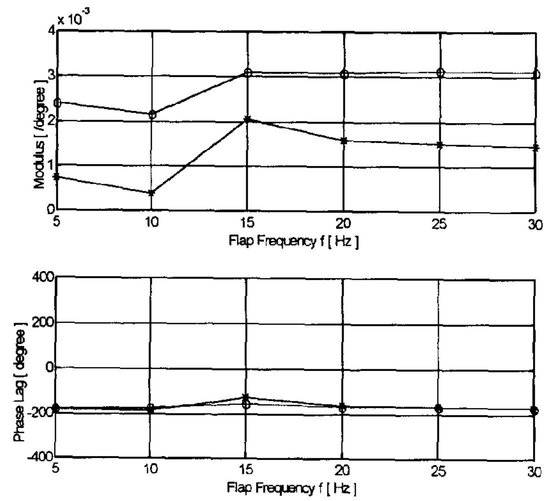

(f) AC100901, M=0.8507, Cm

Figure 8.1 Unsteady Aerodynamic Force Coefficients.
x/c vs Modulus & Phase.
(O: Inboard, ★: Outboard)

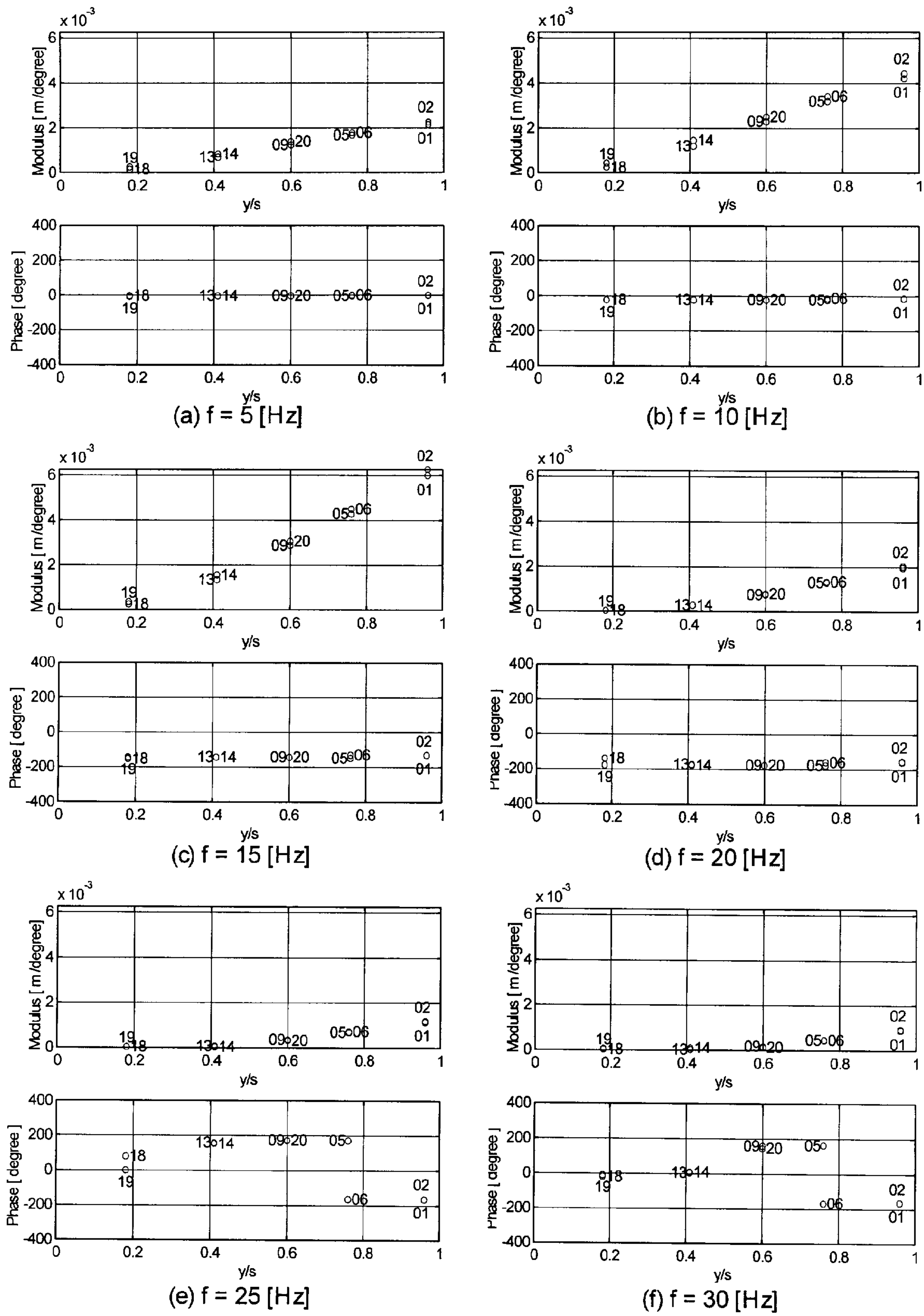

Figure 9.1 Unsteady Model Deformations. x/c vs Modulus & Phase.
Test Case AC100803 M = 0.8002, Po = 79.925 kPa,
Re = 2.142 * 10^7 , Alpha = 0 deg., Delta = 0 deg.